

Golgi twins in late mitosis revealed by genetically encoded tags for live cell imaging and correlated electron microscopy

Guido M. Gaietta*, Ben N. G. Giepmans*[†], Thomas J. Deerinck*, W. Bryan Smith*, Lucy Ngan*, Juan Llopis[‡], Stephen R. Adams[†], Roger Y. Tsien^{†§¶}, and Mark H. Ellisman*^{||}

*National Center for Microscopy and Imaging Research, Center for Research on Biological Structure, and ^{||}Department of Neurosciences, Department Code 0608, University of California at San Diego, La Jolla, CA 92093; [†]Department of Pharmacology and [§]Howard Hughes Medical Institute, Department Code 0648, University of California at San Diego, La Jolla, CA 92093; and [‡]Facultad de Medicina y Centro Regional de Investigaciones Biomédicas, Universidad de Castilla-La Mancha, C/Almansa s/n, 02006 Albacete, Spain

Contributed by Roger Y. Tsien, October 6, 2006 (sent for review August 28, 2006)

Combinations of molecular tags visible in light and electron microscopes become particularly advantageous in the analysis of dynamic cellular components like the Golgi apparatus. This organelle disassembles at the onset of mitosis and, after a sequence of poorly understood events, reassembles after cytokinesis. The precise location of Golgi membranes and resident proteins during mitosis remains unclear, partly due to limitations of molecular markers and the resolution of light microscopy. We generated a fusion consisting of the first 117 residues of α -mannosidase II tagged with a fluorescent protein and a tetracysteine motif. The mannosidase component guarantees docking into the Golgi membrane, with the tags exposed in the lumen. The fluorescent protein is optically visible without further treatment, whereas the tetracysteine tag can be reduced acutely with a membrane-permeant phosphine, labeled with ReAsH, monitored in the light microscope, and used to trigger the photoconversion of diaminobenzidine, allowing 4D optical recording on live cells and correlated ultrastructural analysis by electron microscopy. These methods reveal that Golgi reassembly is preceded by the formation of four colinear clusters at telophase, two per daughter cell. Within each daughter, the smaller cluster near the midbody gradually migrates to rejoin the major cluster on the far side of the nucleus and asymmetrically reconstitutes a single Golgi apparatus, first in one daughter cell and then in the other. Our studies provide previously undescribed insights into Golgi disassociation and reassembly during mitosis and offer a powerful approach to follow recombinant protein distribution in 4D imaging and correlated high-resolution analysis.

cytokinesis | mannosidase | photoconversion | ReAsH | tetracysteine

The Golgi apparatus allows functional diversification of mature proteins by adding and refining carbohydrate chains. In the interphase mammalian cell, the Golgi apparatus is shaped like a ribbon, with stacks of flattened and fenestrated cisternae joined together by a tubular network and anchored in the centrosomal region of the cytoplasm. Before cells enter mitosis, the Golgi apparatus starts a duplication process that may last throughout G₁, S, and G₂, ensuring proper inheritance of the organelle (1, 2). During cell division, it undergoes vesiculation and fragmentation, and its components are found scattered throughout the cytoplasm at metaphase/anaphase in the form of mitotic Golgi clusters and thousands of tiny (\approx 50-nm) vesicles sized below the resolution of light microscopy (LM) (3–9), often referred to as the “Golgi haze.” The nature of the Golgi haze as observed in LM is controversial, with evidence for (6, 10) and against (11–13) coalescence of these vesicular components with the endoplasmic reticulum (ER). From this haze, the Golgi apparatus has been shown to reconstitute, through a series of poorly understood events, reforming the tubules and stacks that are characteristic of its interphase form. Fusions of Golgi-resident enzymes with fluorescent proteins are commonly used

to delineate the Golgi apparatus and follow its dynamics during cell division. However, these fusions are visible only in the LM and usually rely on immunoelectron microscopic approaches for correlated analysis of molecular constituents, with the consequent degradation in quality of the ultrastructural preservation that is associated with antibody labeling (reviewed in ref. 14). To overcome these limitations, we added a small tetracysteine-containing peptide to the carboxyl terminus of green fluorescent protein (GFP) or cyan fluorescent protein (CFP) and fused the resulting fluorescent protein-tetracysteine tag to the first 117 residues of the Golgi resident enzyme α -mannosidase II (MannII). The tetracysteine peptide used in the combinatorial tag, FLNCCPGCCMEP (4C), has an increased affinity and improved ReAsH quantum efficiency compared with earlier tetracysteine peptides (15). The resulting fusion protein, MannII-GFP-4C, was expressed in cultured mammalian cells and used to chronicle the changes occurring to the Golgi apparatus during mitosis. The fluorescent protein allowed for direct live imaging without further labeling, whereas the biarsenical compound ReAsH (15, 16) bound to the tetracysteine component of the tag after acute application of membrane-permeant reducing agents and was used for live cell imaging or for FRET-based photoconversion of diaminobenzidine (DAB) for high-resolution analysis by electron microscopy (EM) (Fig. 1A).

Results

Labeling Tetracysteine Tags with ReAsH-EDT₂ in Oxidizing Environments. MannII-GFP-4C (Fig. 1A and B) was stably expressed in HeLa cells, where it localized in the Golgi apparatus and codistributed with the Golgi proteins Giantin (Fig. 1C), GM-130 (Fig. 1D), and α -mannosidase II (data not shown). The tetracysteine residues in MannII-GFP-4C are exposed to the oxidizing environment of the Golgi lumen and would normally be unavailable to FIASH or ReAsH, because binding of biarsenicals to tetracysteine tags requires the cysteine residues to be completely reduced (17, 18). Thus, when HeLa cells expressing tetracysteine-tagged actin (15), used as a cytoplasmic protein control, and MannII-CFP-4C were incubated with saturating

Author contributions: G.M.G. and B.N.G.G. contributed equally to this work; G.M.G., B.N.G.G., T.J.D., R.Y.T., and M.H.E. designed research; G.M.G., B.N.G.G., T.J.D., W.B.S., and L.N. performed research; J.L. and S.R.A. contributed new reagents/analytic tools; G.M.G., B.N.G.G., T.J.D., W.B.S., R.Y.T., and M.H.E. analyzed data; and G.M.G., B.N.G.G., T.J.D., W.B.S., R.Y.T., and M.H.E. wrote the paper.

The authors declare no conflict of interest.

Freely available online through the PNAS open access option.

Abbreviations: CFP, cyan fluorescent protein; DAB, diaminobenzidine; EM, electron microscopy; ER, endoplasmic reticulum; LM, light microscopy; MannII, α -mannosidase II; TBP, tributylphosphine; TEP, triethylphosphine.

[¶]To whom correspondence should be addressed. E-mail: rtsien@ucsd.edu.

© 2006 by The National Academy of Sciences of the USA

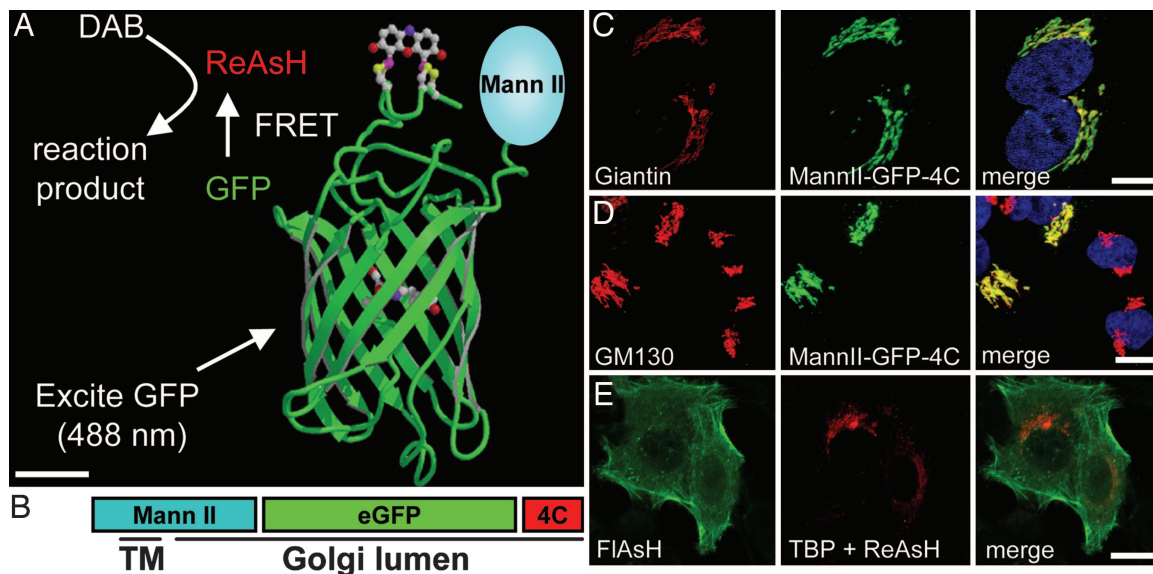


Fig. 1. Construction and validation of a Golgi marker for EM and LM imaging. (A) Generation of a combinatorial tag by using GFP and a tetracycysteine motif and application to correlated LM/EM. FRET between GFP and ReAsH was used to trigger photoconversion of DAB. Because FRET exclusively occurs between closely apposed fluorochromes, only the biarsenical bound to 4C will accept the energy from GFP and produce singlet oxygen, thereby increasing the specificity of photoconversion. (Scale bar: ≈ 1 nm.) Note that the structure of the tetracycysteine is a model, not an experimental determination. (B) The Emerald GFP-4C (eGFP-4C) module was fused to the 117 N-terminal residues of MannII containing cytoplasmic, transmembrane, and part of the intraluminal domains. (C and D) MannII-GFP-4C localizes specifically to the Golgi apparatus. HeLa cells stably expressing MannII-GFP-4C (green) were labeled with an antibody to Giantin (C, red), an integral component of the Golgi membrane, or GM-130 (D, red), a protein of the Golgi matrix. (Scale bars: $10 \mu\text{m}$.) (E) The intraluminal tetracycysteine tag is labeled only in reducing conditions. HeLa cells transiently expressing cytoplasmic tetracycysteine-tagged actin and Golgi resident MannII-CFP-4C were labeled with FIAsh-EDT₂ in the absence of TBP. FIAsh bound to the reduced thiols in tetracycysteine-tagged actin but not to the Golgi-luminal oxidized thiols in MannII-CFP-4C. Next, cells were treated simultaneously with ReAsH-EDT₂ and the membrane-permeant reducing agent, TBP. TBP transiently reduces the intraluminal tetracycysteine and, thus, allows ReAsH binding. (Scale bar: $20 \mu\text{m}$.)

concentrations of FIAsh-EDT₂ in absence of tributylphosphine (TBP), only actin was labeled (Fig. 1E Left). Coadministration of membrane-permeant reducing agents TBP or triethylphosphine (TEP) allowed ReAsH labeling of MannII-CFP-4C in the Golgi lumen of living cell (Fig. 1E Middle and Right). CFP rather than GFP was used here because of spectral overlap between FIAsh and GFP.

MannII-GFP-4C Distribution During Mitosis: Correlated Microscopy and FRET-Based Photoconversion. To examine the Golgi disassembly and partitioning during mitosis in correlated LM and EM studies, we labeled cells stably expressing MannII-GFP-4C with ReAsH-EDT₂ in the presence of TEP, imaged multiple fields by using a high-speed, two photon laser-scanning microscope equipped with a motorized stage, and then photoconverted the imaged areas (Fig. 2). We examined the progression through cell division by using the maximum intensity projection of MannII-GFP-4C (GFP fluorescence displayed in negative contrast) (Fig. 2A; see Movie 1, which is published as supporting information on the PNAS web site). This experimental setup allowed us to record multiple fields in parallel over long periods of time (i.e., days), capturing cells at different stages of division. We preferred this approach to chemical treatments aimed at synchronizing the cell population at a specific mitotic stage, which might lead to alterations of the Golgi apparatus, cellular hypertrophy, and artifacts in the distribution and dynamics of Golgi proteins. Upon completion of live imaging, sometimes when a critical stage of mitosis was seen, cells were fixed with 2% glutaraldehyde and processed for photoconversion of DAB (Fig. 2B–E). Photoexcitation of ReAsH generates singlet oxygen, which locally polymerizes DAB into a fine precipitate that is subsequently rendered electron-dense by treatment with osmium tetroxide (19). Here, we indirectly excited ReAsH through FRET from GFP (Fig. 1A). The electron-dense product was

found localized to the medial and trans-Golgi stacks, with traces in the cis-Golgi stacks of interphase cells. This is a distribution similar to that reported by others for the native form of α -mannosidase II in HeLa (20) and other (21) cells. The nucleus, nuclear envelope, ER, and mitochondria were not labeled (Fig. 2F). MannII-GFP-4C was found at prophase (Fig. 2G and H) and prometaphase (Fig. 2I and J) in vesicles and clusters similar in size and morphology to those described (3, 4, 6, 7, 9), which were generally separated from the membranes of the rough ER. At late metaphase, the majority of the fusion protein was found in small vesicles ranging from 50 to 70 nm (as described in refs. 4 and 7), and distributed at the periphery or close to the metaphase plate (Fig. 2K–M; see Movie 2, which is published as supporting information on the PNAS web site). In our initial time-lapse studies, total fluorescence was seemingly less during mitosis. Movement out of the defined Z sections due to the cell rounding was found to cause this effect. The total GFP fluorescence is nonetheless conserved even though the haze looks much dimmer than the organized Golgi stacks (see below). We found the vesicles along the metaphase plate to be clearly separated from ER tubules (Fig. 2K), whereas those at the cell poles were sometimes close to ER-like membranes (Fig. 2L and M).

Appearance of Four Golgi Clusters at Telophase. According to descriptions in refs. 22 and 23, the Golgi haze coalesces into one ribbon-like structure after the daughter cells have undergone abscission. In time-lapse recordings of HeLa cells expressing mCherry- α -tubulin and MannII-GFP-4C (Fig. 3A; see Movie 3, which is published as supporting information on the PNAS web site) or high-resolution imaging of HeLa cells stably expressing MannII-GFP-4C (Fig. 3B and C; see Movies 4 and 5, which are published as supporting information on the PNAS web site), we saw that twin clusters of vesicles and tubular structures containing MannII-GFP-4C consistently formed at the edge of the

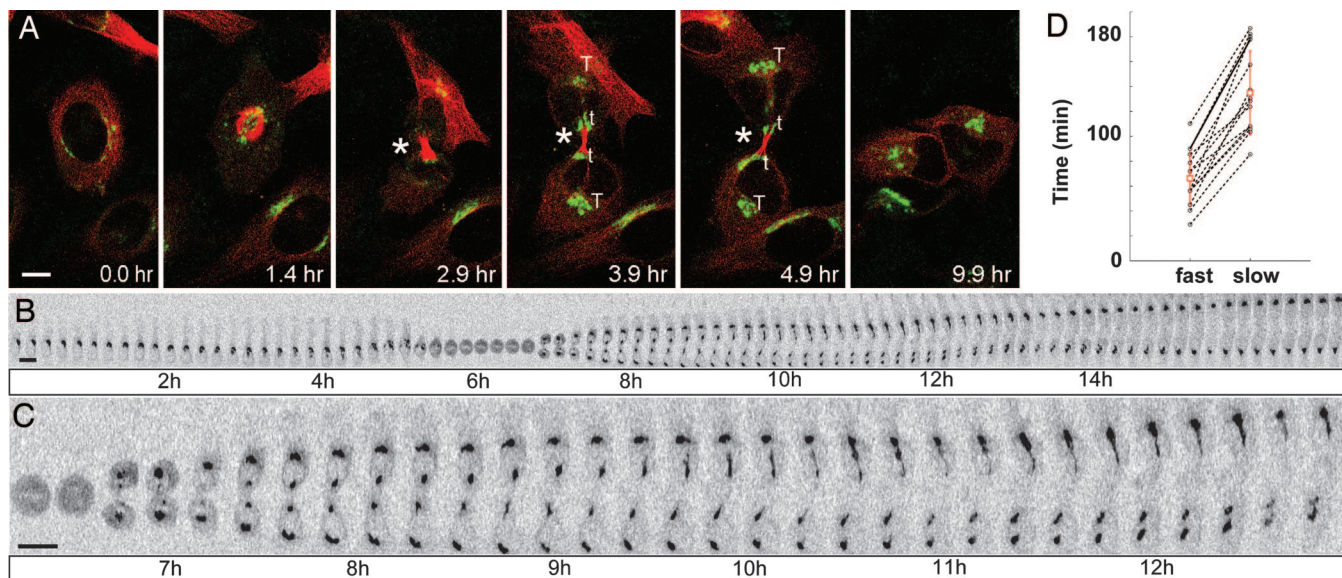


Fig. 3. Four Golgi twins appear in telophase. (A) Golgi twins assemble at the midbody. HeLa cells expressing mCherry- α -tubulin (red) and MannII-GFP-4C (green) were imaged every 10 min. Major ("T") and minor ("t") Golgi twins appeared at the midbody (marked by a white asterisk) at late telophase cytokinesis (Movie 3). (Scale bar: 10 μ m.) (B and C) Seventeen (B) and 7 h (C) zoomed kymograph (where the sequential regions of interests from the time-lapse recording are fused together to show dynamic changes in a 2D representation) of the sum intensity projection (inverted contrast) of the GFP fluorescence in a dividing cell. Cells were imaged every 8 min for 17 h every 0.25 μ m (the total thickness is 34 μ m; Movie 5; a higher spatiotemporal resolution imaging in one Z plane can be found in Movie 6). (Scale bar: 20 μ m.) (D) Kinetics of Golgi twin coalescence. $t = 0$ was defined as the time when four Golgi clusters were clearly visible, and reconstitution was considered complete when 95% of the fluorescence in each daughter cell (as defined by 3D isosurface renderings) was contiguous. In 15 of 15 cell pairs observed, the rate of reconstitution was twice as fast in one daughter cell as compared with the other (mean fast = 66 ± 22 min; mean slow = 135 ± 34 min; $P < 0.001$, t test). The solid black line refers to values collected for the cell displayed in the kymograph in B and C.

almost 2 h for those containing the faster twins, and from 1 to >3 h for those containing the slower twins. Independently from the variability in total time, the coalescence differs by 2-fold between daughter cells.

EM Analysis of Golgi Twins. Transmitted light, GFP, and ReAsH images were recorded in time-lapse from live cells (Fig. 4*A Top*, *Middle*, and *Bottom*, respectively; see Movie 7, which is published as supporting information on the PNAS web site). When the Golgi twins were clearly distinguishable by fluorescence, cells were fixed, photoconverted, and processed for EM. Thin sections of the epoxy-embedded samples were used to examine the contact region between two daughter cells (Fig. 4*B–D*). MannII-GFP-4C localized in vesicles and vesicle-tubular structures closely apposed to the microtubules of the midbody (Fig. 4*C*) and to the microtubules stretching between the midbody and the centrosphere (Fig. 4*D*; see Figs. 5 and 6, which are published as supporting information on the PNAS web site). Similar observations were made at lower resolution in HeLa cells expressing MannII-GFP-4C fixed and stained for α -tubulin (Fig. 4*E* and *F*).

Discussion

The ability to precisely localize target proteins with high spatial and temporal resolution is fundamental in understanding dynamic events in cell biology. The combination of multiple molecular tags is advantageous for this purpose, as we showed in our study on Golgi apparatus behavior during mitosis. Golgi-resident proteins tagged with GFP have been extensively used to study the disassembly and reassembly of the Golgi apparatus by live imaging. Although this approach is relatively easy to set up and can be extended to functional studies, it lacks the resolution required to resolve the mitotic haze, when Golgi residents are in the thousands of 50- to 70-nm vesicles scattered throughout the cytoplasm of the dividing cell. Because GFP is not directly visible in the electron microscope, traditional immunocytochemistry

approaches for correlative light/electron microscopy studies must be used. By appending a tetracysteine motif to the carboxyl terminus of GFP and using this combinatorial tag in a fusion with a Golgi resident protein, we generated a multiresolution marker that allowed us to merge fluorescence live-imaging studies and ultrastructural analysis. The sequence FLNCCPGCCMEP belongs to the latest series of enhanced tetracysteine motifs, which have higher fluorescence quantum yields (ReAsH quantum yield on GFP = 0.42–0.47), improved dithiol resistance, and higher contrast. We further increased the absolute contrast of ReAsH fluorescence and photoconversion by fusing the tetracysteine motif to GFP and exciting the biarsenical by FRET from the donor fluorescent protein (15). Because the distance between acceptor and donor must be within ≈ 8 nm, only the biarsenical bound to GFP-4C is excited by FRET, whereas the nonspecific biarsenicals are disfavored. Because cells were fixed after labeling with ReAsH and no antibodies were needed to paint the studied structures, we were able to use high concentrations (2%) of a strong cross-linking fixative (glutaraldehyde), which allowed optimal preservation of the ultrastructure.

Recovery of Binding in Oxidizing Compartments by Brief Reduction.

Biarsenical binding to an oxidized tetracysteine motif is recovered by acute application of a reducing agent (16). We showed that recovery is possible even if the tetracysteine motif is located intraluminally in an oxidizing cellular compartment, such as the Golgi apparatus or the ER. The only limiting factor in this case is the use of a membrane-permeant reducing agent, such as TEP or TBP. The requirement for reduction of the thiol groups in the cysteines actually can be used to our advantage to sequentially label two tetracysteine-tagged proteins localized in cellular compartments with different redox values. As shown in Fig. 1*E*, tetracysteine-tagged actin and MannII-GFP-4C are labeled with FlAsH and ReAsH, respectively, without cross interference.

popular tags in the past decade, yet their use has been limited to fluorescence microscopy. Here, we demonstrate the application of a more versatile tagging system, extend its applicability to intracellular sites inside the lumen of oxidizing environments, and demonstrate that such capabilities have value for basic studies of the complex dynamics of intracellular organelle systems, such as the Golgi apparatus. The fusion of an intrinsically fluorescent protein and a tetracysteine motif is a relatively simple enhancement that will allow researchers to take advantage of a widely used tag with high fluorescent quantum yield and excellent contrast (GFP and derivatives) and the adaptability of the small tetracysteine tag system and the biarsenicals ligands that bind selectively to these domains.

Materials and Methods

In Vivo Labeling in Reducing Environments. Cells stably expressing MannII-GFP-4C were labeled for 1 h at 37°C with 1.25 μ M ReAsH-EDT₂/10 μ M EDT/1 mM TEP in Hank's Balanced Salt Solution with D⁺ glucose (1 g/liter). One molar solutions of TBP and TEP were prepared fresh in ethanol and diluted 1:1,000 in HBSS before the addition of ReAsH-EDT₂ and EDT. Free and nonspecifically bound ReAsH was removed by washing with EDT (600 μ M).

1. Hager KM, Striepen B, Tilney LG, Roos DS (1999) *J Cell Sci* 112:2631–2638.
2. Jackowski S (1996) *J Biol Chem* 271:20219–20222.
3. Lucoq JM, Pryde JG, Berger EG, Warren G (1987) *J Cell Biol* 104:865–874.
4. Lucoq JM, Berger EG, Warren G (1989) *J Cell Biol* 109:463–474.
5. Pypaert M, Nilsson T, Berger EG, Warren G (1993) *J Cell Sci* 104:811–818.
6. Zaal KJ, Smith CL, Polishchuk RS, Altan N, Cole NB, Ellenberg J, Hirschberg K, Presley JF, Roberts TH, Siggia E, *et al.* (1999) *Cell* 99:589–601.
7. Jokitalo E, Cabrera-Poch N, Warren G, Shima DT (2001) *J Cell Biol* 154:317–330.
8. Misteli T, Warren G (1995) *J Cell Sci* 108:2715–2727.
9. Shima DT, Haldar K, Pepperkok R, Watson R, Warren G (1997) *J Cell Biol* 137:1211–1228.
10. Lippincott-Schwartz J, Zaal KJ (2000) *Histochem Cell Biol* 114:93–103.
11. Warren G (1993) *Annu Rev Biochem* 62:323–348.
12. Pecot MY, Malhotra V (2004) *Cell* 116:99–107.
13. Nunnari J, Walter P (1996) *Cell* 84:389–394.
14. Giepmans BN, Adams SR, Ellisman MH, Tsien RY (2006) *Science* 312:217–224.
15. Martin BR, Giepmans BN, Adams SR, Tsien RY (2005) *Nat Biotechnol* 23:1308–1314.
16. Adams SR, Campbell RE, Gross LA, Martin BR, Walkup GK, Yao Y, Llopis J, Tsien RY (2002) *J Am Chem Soc* 124:6063–6076.
17. Griffin BA, Adams SR, Tsien RY (1998) *Science* 281:269–272.
18. Griffin BA, Adams SR, Jones J, Tsien RY (2000) *Methods Enzymol* 327:565–578.
19. Gaietta G, Deerinck TJ, Adams SR, Bouwer J, Tour O, Laird DW, Sosinsky GE, Tsien RY, Ellisman MH (2002) *Science* 296:503–507.
20. Rabouille C, Hui N, Hunte F, Kieckbusch R, Berger EG, Warren G, Nilsson T (1995) *J Cell Sci* 108:1617–1627.
21. Velasco A, Hendricks L, Moremen KW, Tulsiani DR, Touster O, Farquhar MG (1993) *J Cell Biol* 122:39–51.
22. Shima DT, Cabrera-Poch N, Pepperkok R, Warren G (1998) *J Cell Biol* 141:955–966.
23. Seemann J, Pypaert M, Taguchi T, Malsam J, Warren G (2002) *Science* 295:848–851.
24. Moskalewski S, Thyberg J (1990) *J Submicrosc Cytol Pathol* 22:159–171.
25. Thyberg J, Moskalewski S (1992) *J Submicrosc Cytol Pathol* 24:495–508.
26. Thyberg J, Moskalewski S (1998) *Microsc Res Tech* 40:354–368.
27. Thyberg J, Moskalewski S (1999) *Exp Cell Res* 246:263–279.
28. Uchiyama K, Jokitalo E, Lindman M, Jackman M, Kano F, Murata M, Zhang X, Kondo H (2003) *J Cell Biol* 161:1067–1079.
29. Piel M, Nordberg J, Euteneuer U, Bornens M (2001) *Science* 291:1550–1553.

Photoconversion of DAB and Electron Microscopy. ReAsH-labeled cells were fixed in 2% glutaraldehyde in sodium cacodylate buffer (0.1 M, pH 7.4), and the microscope stage was switched from 37°C to 4°C. After 20 min, the cells were rinsed in cacodylate buffer and treated for 5 min with blocking buffer: 10 mM KCN/10 mM aminotriazole/0.01% hydrogen peroxide/50 mM glycine in 0.1 M cacodylate buffer (19). This buffer was replaced with blocking buffer, including 1 mg/ml DAB, and photoconversion was performed by using intense illumination (75 W xenon lamp without neutral density filters) focused through the microscope objective. Washing and further preparation for EM were performed as described in ref. 19.

Supporting Information. Additional details can be found in *Supporting Materials and Methods*, which is published as supporting information on the PNAS web site.

We thank Junru Hu for skillful technical assistance; Sunny Chow, Hiroyuki Hakozaki, and Fan Chang for help with the live imaging setup and the data processing; and Brent Martin for the retroviral expression vectors with the improved tetracysteine motif. This work was supported by National Institutes of Health Grants 2P41RR004050-16 (to M.H.E.) and GM72033 (to R.Y.T.).